Optical excitations in electroluminescent polymers: the poly(***para***-phenylenevinylene) family

1997 J. Phys.: Condens. Matter 9 5989

(http://iopscience.iop.org/0953-8984/9/27/024)

J. Phys.: Condens. Matter **9** (1997) 5989–6000. Printed in the UK PII: S0953-8984(97)83399-1

Optical excitations in electroluminescent polymers: the poly(*para*-phenylenevinylene) family

Kikuo Harigaya†

Physical Science Division, Electrotechnical Laboratory, Umezono 1-1-4, Tsukuba, Ibaraki 305, Japan

Received 14 April 1997

Abstract. The components of photoexcited states with large spatial extent in the optical absorption spectra of the electroluminescent conjugated polymers are investigated by using the intermediate-exciton theory. We calculate the ratio of the oscillator strengths due to long-range excitons to the sum of all of the oscillator strengths of the absorption, as a function of the monomer number. The oscillator strengths of the long-range excitons in poly(*para*-phenylene) are smaller than those for poly(*para*-phenylenevinylene), and those for poly(*para*-phenylene-divinylene) are larger than those for poly(*para*-phenylenevinylene). Such relative variations are explained by the differences of the numbers of vinylene units. The oscillator strengths of long-range excitons in poly(di-*para*-phenylenevinylene) are much larger than those for the above three polymers, due to the increase of the number of phenyl rings. We also find that the energy positions of the almost localized excitons are is nearly the same in the four polymers.

1. Introduction

The observation of remarkable electroluminescent properties of the polymer poly(*para*-phenylenevinylene) (PPV) [1] has attracted physical and chemical research activity. An important recent development is the observation of stimulated emission and lasing from a PPV layer incorporated within an optical cavity [2]. Lasing has also been proposed in order to explain the band narrowing observed on high-intensity photoexcitation of a composite film of a PPV derivative and nanoparticles of TiO_2 [3]. Therefore, obtaining an understanding of the structures of photoexcited states in PPV and related polymers containing phenyl rings is an interesting research topic.

In the PPV polymer, the onset of the photocurrents is located at an excitation energy between 3.0 eV and 4.0 eV [4–6], and this energy is significantly larger than both that of the optical absorption edge at about 2.0 eV and that of the lowest peak energy at 2.4 eV. In a previous study [7, 8], we have characterized the extent of the photoexcited states of the PPV by using the intermediate-exciton theory. When the distance between an electron and a hole is shorter than the spatial extent of the monomer, we have called the exciton a 'short-range' exciton. When the exciton width is larger than the extent of the monomer, we have called the exciton a 'long-range' exciton. We have characterized each photoexcited state as 'short-range' or 'long-range'. We have shown that the long-range exciton feature starts at an energy on the higher-energy side of the lowest feature of the optical absorption of PPV. The energy position is nearly the same as that of the semiconducting energy gap,

† E-mail address: harigaya@etl.go.jp; URL: http://www.etl.go.jp/People/harigaya/.

0953-8984/97/275989+12$19.50

which has been interpreted as the onset of the large photocurrents observed in experiments. Therefore, the presence of photoexcited states with large spatial extent is essential in the mechanisms of the remarkable photocurrents observed in PPV.

The purpose of this paper is to look at contributions from long-range excitons, which here large effects on the photoconduction properties in PPV-related polymers: poly(*para*-phenylene) (PPP), poly(*para*-phenylenedivinylene) (PPD), and poly(di-*para*-phenylenevinylene) (PDV). The structures of these polymers—namely, the PPV family—are illustrated in figure 1. These polymers are composed of phenyl rings and vinylene CH dimers. The names of the two polymers and their abbreviations, PPD and PDV, are 'pseudonyms' (tentative names) in this paper, because common names of these polymers are not established at present. The long-range excitons are characterized as we have done for PPV in the previous study [7, 8].

In the next section, the theoretical formalism is explained, and the characterization method for the long-range excitons is given. The calculated results are reported in section 3, and the paper is concluded with a summary in section 4.

2. The model

We consider the following model with electron–phonon and electron–electron interactions.

$$H = H_{\rm pol} + H_{\rm int} \tag{1}$$

$$H_{\rm pol} = -\sum_{\langle i,j\rangle,\sigma} (t - \alpha y_{i,j})(c^{\dagger}_{i,\sigma} c_{j,\sigma} + {\rm HC}) + \frac{K}{2}\sum_{\langle i,j\rangle} y^2_{i,j} \tag{2}$$

$$H_{\rm int} = U\sum_i \left(c^{\dagger}_{i,\uparrow}c_{i,\uparrow} - \frac{n_{\rm el}}{2}\right)\left(c^{\dagger}_{i,\downarrow}c_{i,\downarrow} - \frac{n_{\rm el}}{2}\right) + \sum_{i,j} W(r_{i,j})\left(\sum_{\sigma} c^{\dagger}_{i,\sigma}c_{i,\sigma} - n_{\rm el}\right)\left(\sum_{\tau} c^{\dagger}_{j,\tau}c_{j,\tau} - n_{\rm el}\right). \tag{3}$$

In equation (1), the first term $H_{\rm pol}$ is the tight-binding model along the polymer backbone with electron–phonon interactions which couple electrons with modulation modes of the bond lengths, and the second term $H_{\rm int}$ is the potential describing the Coulomb interaction among the electrons. In equation (2), t is the hopping integral for the nearest-neighbour carbon atoms in the ideal system without bond alternations; α is the electron–phonon coupling constant that modulates the hopping integral linearly with respect to the bond variable $y_{i,j}$ which measures the magnitude of the bond alternation of the bond $\langle i, j\rangle$; $y_{i,j} > 0$ for longer bonds and $y_{i,j} < 0$ for shorter bonds (the average of $y_{i,j}$ is taken to be zero); K is the harmonic spring constant for $y_{i,j}$; and the sum is taken over the pairs of neighbouring atoms. Equation (3) describes the Coulomb interactions among electrons. Here, $n_{\rm el}$ is the average number of electrons per site; $r_{i,j}$ is the distance between the ith and jth sites; and

$$W(r) = \frac{1}{\sqrt{(1/U)^2 + (r/aV)^2}} \tag{4}$$

is the parametrized Ohno potential. The quantity $W(0) = U$ is the strength of the on-site interaction; V is the strength of the long-range part ($W(r) \sim aV/r$ in the limit $r \gg a$); and $a = 1.4$ Å is the mean bond length. The parameter values used in this paper are $\alpha = 2.59t$ Å^{-1}, $K = 26.6t$ Å^{-2}, $U = 2.5t$, and $V = 1.3t$. They have been determined by comparison with experiments on PPV, and have been used in [7, 8]. Most of the quantities in energy units are given in units of t in this paper.

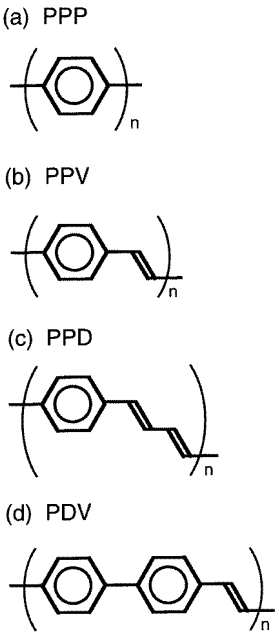

Figure 1. Lattice structures of the electroluminescent polymers studied in this paper. The abbreviations, PPD and PDV, are 'pseudonyms'.

The excitation wavefunctions of the electron–hole pair are calculated by using the Hartree–Fock approximation followed by the single-excitation configuration interaction method. This method, which is appropriate for cases of moderate Coulomb interactions—strengths between negligible and strong Coulomb interactions—is known as the intermediate-exciton theory in the literature [7, 8]. We write the singlet electron–hole excitations as

$$|\mu, \lambda\rangle = \frac{1}{\sqrt{2}}(c^{\dagger}_{\mu,\uparrow}c_{\lambda,\uparrow} + c^{\dagger}_{\mu,\downarrow}c_{\lambda,\downarrow})|g\rangle \tag{5}$$

where μ and λ stand for unoccupied and occupied states, respectively, and $|g\rangle$ is the Hartree–Fock ground state. The general expression for the κth optical excitation is

$$|\kappa\rangle = \sum_{(\mu,\lambda)} D_{\kappa,(\mu,\lambda)}|\mu, \lambda\rangle. \tag{6}$$

After inserting the relation with the site representation $c_{\mu,\sigma} = \sum_i \alpha_{\mu,i}c_{i,\sigma}$, we obtain

$$|\kappa\rangle = \frac{1}{\sqrt{2}}\sum_{(i,j)} B_{\kappa,(i,j)}(c^{\dagger}_{i,\uparrow}c_{j,\uparrow} + c^{\dagger}_{i,\downarrow}c_{j,\downarrow})|g\rangle \tag{7}$$

where

$$B_{\kappa,(i,j)} = \sum_{(\mu,\lambda)} D_{\kappa,(\mu,\lambda)}\alpha^{*}_{\mu,i}\alpha_{\lambda,j}. \tag{8}$$

Thus, $|B_{\kappa,(i,j)}|^2$ is the probability that an electron locates at the ith site and a hole is at the jth site.

We shall define the following quantity:

$$P_{\kappa} = \sum_{i\in M}\sum_{j\in M}|B_{\kappa,(i,j)}|^2 \tag{9}$$

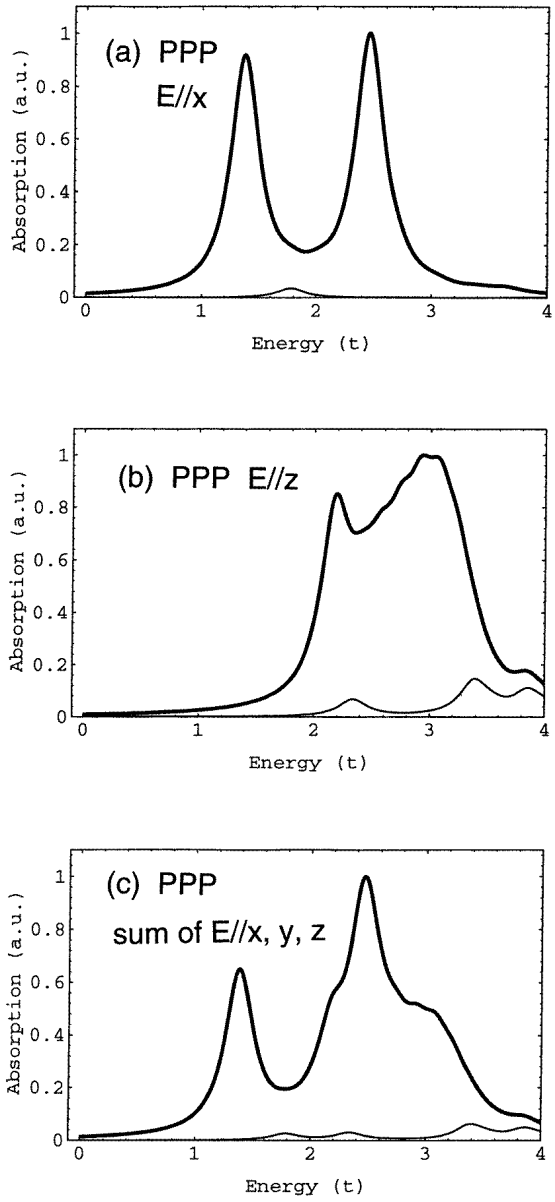

Figure 2. Optical absorption spectra of the PPP. The polymer is in the x–z plane, and its axis is parallel to the x-axis. The electric field of the light is parallel to the chain and in the direction of the x-axis in (a), and it is perpendicular to that axis and along the z-axis in (b). The orientationally averaged spectra are shown in (c). The number of PPP units is $N_{\rm m} = 19$. The bold line is for the total absorption. The thin line indicates the absorption of the long-range component. The Lorentzian broadening $\gamma = 0.15t$ is used.

where M is a set of sites within a single monomer—in other words, a set of carbon sites included in the brackets of each polymer shown in figure 1. When $P_\kappa > 1/N_{\rm m}$ ($N_{\rm m}$ is the number of monomers used in the calculations for periodic polymer chains), the electron

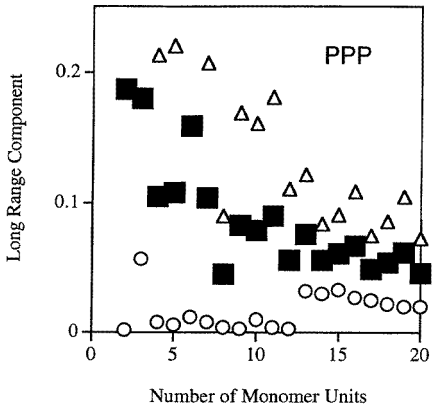

Figure 3. The long-range components of the optical absorption spectra as functions of the PPP unit number N_m. The squares are for the total absorption. The circles and triangles indicate the data for the cases with the electric field parallel and perpendicular to the polymer axis, respectively.

and hole favour large amplitudes in the same single monomer. Then, this excited state is identified as a short-range exciton. On the other hand, when $P_\kappa < 1/N_m$, the excited state is characterized as a long-range exciton. This characterization method is performed for all of the photoexcited states $|\kappa\rangle$, and a long-range component in the optical absorption spectrum is extracted from the total absorption. In the next section, the numerical results will be reported, and a discussion will be given.

3. Long-range excitons in the PPV family

3.1. PPP and PPV

We discuss the properties of photoexcited states in PPP (figure 1(a)) and PPV (figure 1(b)) in this subsection. The numerical results for PPV have been given in references [7, 8] already, but they are given again for comparing with the results for PPP. Figures 2 and 3 show the optical absorption spectra and the long-range components of the oscillator strengths for PPP, and figures 4 and 5 show the results for PPV.

Figures 2(a) and 2(b) show the anisotropies of the optical absorption of PPP. The electric field of the light is parallel and perpendicular to the polymer axis in figures 2(a) and 2(b), respectively. The thin lines show the contributions from long-range excitons. In figure 2(a), there are two features centred at around about $1.4t$ and $2.5t$. The former comes from optical excitations between the highest occupied molecular orbital (HOMO) and the lowest unoccupied molecular orbital (LUMO). The HOMO and LUMO have certain magnitudes of dispersions near the Brillouin zone centre, and therefore the excitons near the energy $1.4t$ have an appreciable long-range component. In fact, we observe a peak due to long-range excitons at around the energy $1.8t$. On the other hand, the feature at around $2.5t$ is due to transitions between spatially localized band states [9]. So, this feature does not have an appreciable long-range component on the higher-energy side of the peak. Next, we discuss the case with a perpendicular electric field shown in figure 2(b). There is a feature at $2.2t$, whose long-range exciton component exists on the higher-energy side. At energies higher than that of this feature, several transitions are mixed, and the long-range component is

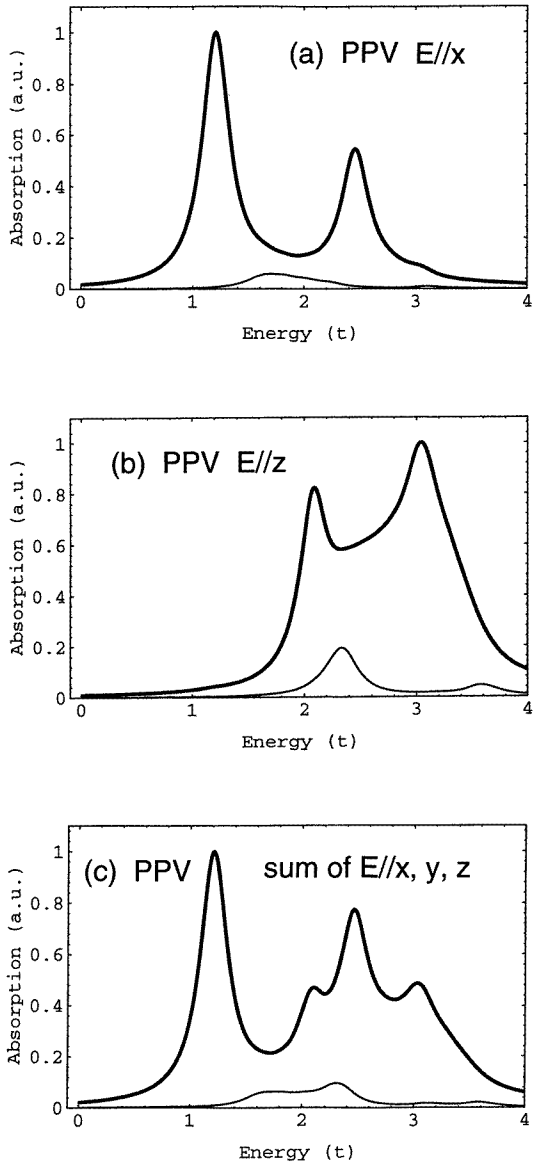

Figure 4. Optical absorption spectra of the PPV. The polymer is in the x–z plane, and its axis is parallel to the x-axis. The electric field of the light is parallel to the chain and in the direction of the x-axis in (a), and it is perpendicular to that axis and along the z-axis in (b). The orientationally averaged spectra are shown in (c). The number of PPV units is $N_{\rm m} = 20$. The bold line is for the total absorption. The thin line indicates the absorption of the long-range component. The Lorentzian broadening $\gamma = 0.15t$ is used.

dominant for energies larger than $3.0t$. Figure 2(c) shows the absorption spectra where the direction of the electric field of light is orientationally averaged. We find that two features at around $1.4t$ and $2.5t$ in the parallel-electric-field case give the two central peaks in the spectra. The features in the perpendicular-field case overlap with the lower- and

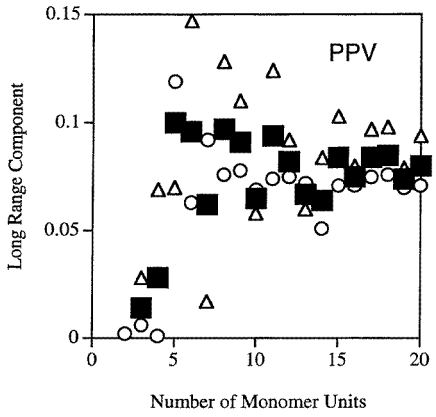

Figure 5. The long-range components of the optical absorption spectra as functions of the PPV unit number N_m. The squares are for the total absorption. The circles and triangles indicate the data for the cases with the electric field parallel and perpendicular to the polymer axis, respectively.

higher-energy sides of the dominant feature at around $2.5t$.

Figure 3 summarizes the long-range components of the oscillator strengths of PPP. They are shown as functions of the PPP monomer number N_m. The squares are for the total absorption. The circles and triangles indicate the data for the cases with the electric field parallel and perpendicular to the polymer axis, respectively. Generally, the long-range component of the perpendicular-electric-field case is larger than that of the parallel-field case. It seems that the long-range component of the orientationally averaged spectra saturates at approximately 7% near $N_m = 20$. Note that the small fluctuations of the plots with respect to N_m are due to the numerical calculation errors, and are not intrinsic behaviour. Such numerical fluctuations have also been seen in our previous work on PPV [7, 8]. It is suggested that readers look at the overall variations of the long-range component with respect to N_m.

Next, we compare the results on PPP with those on PPV. The numerical absorption spectra are shown in figure 4, and their long-range components are shown in figure 5. The results have already been reported in [7, 8], but they are shown again in order to allow a comparison with the results for the other polymers. Comparing figure 2 with figure 4, we observe that the peak structures of PPP and PPV are similar at first glance. However, there is a quantitative difference: the oscillator strengths of the lowest excitation in figure 4(a) and that in figure 4(c) are larger for PPV than those for PPP. The long-range component of the lowest exciton is larger for PPV, too. This fact is reflected in the saturated value of the total long-range component of PPV shown in figure 5 being larger than that of PPP shown in figure 3.

As noted in reference [9], the lowest optical excitations of PPP and PPV have characters like those of excitons in a simple prototype polymer: *trans*-polyacetylene. The band structures of polyacetylene are well described by the Su–Schrieffer–Heeger (SSH) model [10]. The quasiparticle band structures have finite dispersions at the top (bottom) of the valence band (conduction band). Therefore, the lowest exciton owing to these dispersive bands has an apparent long-range component on the higher-energy side after taking account of the Coulomb interactions among electrons. The lowest excitons of PPP and PPV have similar characters, and thus figures 2(a) and 4(a) show the dominant contributions of long-

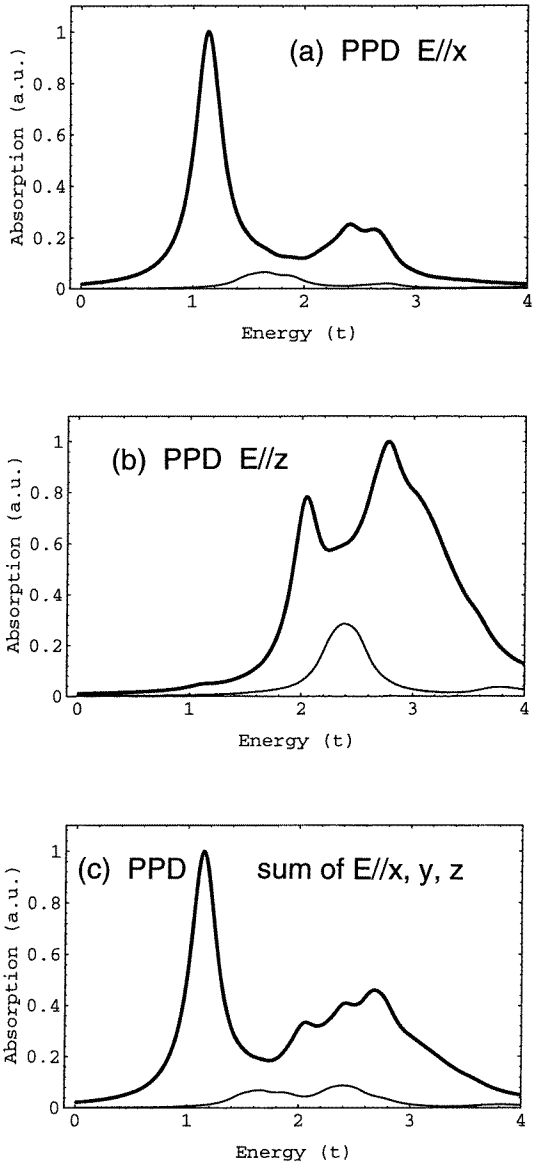

Figure 6. Optical absorption spectra of the PPD. The polymer is in the x–z plane, and its axis is parallel to the x-axis. The electric field of the light is parallel to the chain and in the direction of the x-axis in (a), and it is perpendicular to that axis and along the z-axis in (b). The orientationally averaged spectra are shown in (c). The number of PPD units is $N_{\rm m} = 12$. The bold line is for the total absorption. The thin line indicates the absorption of the long-range component. The Lorentzian broadening $\gamma = 0.15t$ is used.

range excitons with respect to the lowest band-to-band optical excitations.

The difference between the polymer structures of PPP and PPV in figures 1(a) and 1(b) is that a vinylene bond is added between the phenyl rings of PPP. This is related to the property that the electronic structures near the energy gap of PPV have more dispersive

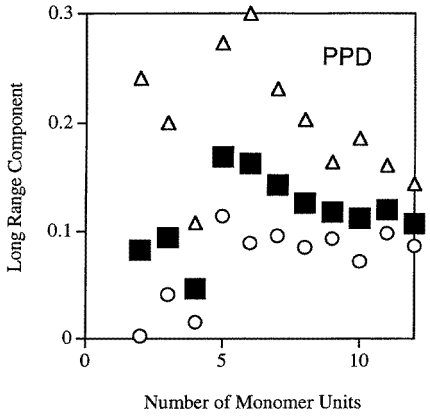

Figure 7. The long-range components of the optical absorption spectra as functions of the PPD unit number N_m. The squares are for the total absorption. The circles and triangles indicate the data for the cases with the electric field parallel and perpendicular to the polymer axis, respectively.

characters than those of PPP, and thus the optical excitations owing to these bands will more closely resemble those of *trans*-polyacetylene described by the SSH model. Therefore, the relative oscillator strengths of the lowest excitons of PPV (figure 4(a)) are larger than those of PPP (figure 2(a)). Also, the total long-range component (about 8%) of PPV (figure 5) is larger than that (about 7%) of PPP (figure 3). We could say that the optical excitations of PPV will have photoconductive properties which are stronger than those of PPP.

3.2. PPD

For PPD, as shown in figure 1(c), there are two vinylene bonds between the neighbouring phenyl rings. In this subsection, we look at the optical properties resulting from electronic structures and excitonic effects of PPD.

Figure 6 shows the optical absorption spectra, when the electric field of the light is parallel to the polymer axis (figure 6(a)), perpendicular to the polymer (figure 6(b)), and is averaged over orientations (figure 6(c)). Long-range exciton contributions are also shown in these three figures. When the electric field is along the polymer axis (figure 6(a)), the oscillator strengths of the lowest exciton at around the energy $1.2t$ are dominant. This feature has its long-range component on the higher-energy side. There is a small feature at around the energy $2.5t$. The oscillator strengths of this feature become smaller than those of PPV shown in figure 4(a). The lowest exciton feature becomes larger than that of figure 4(a). This arises from the number of vinylene units in PPD being larger than that for PPV. When the electric field is perpendicular to the polymer (figure 6(b)), the overall spectral shape is similar to that in figure 4(b). Figure 6(c) shows the orientationally averaged spectra. The lowest exciton feature becomes more dominant on going from PPP (figure 2(c)) to PPV (figure 4(c)) to PPD. The three-peak structure from $\sim 2t$ to $\sim 3t$ is commonly seen in these three polymers, but their oscillator strengths become weaker.

Figure 7 shows the long-range components of PPD as functions of the monomer number N_m. The maximum value of N_m is 12. The value of N_m at which the saturation behaviour

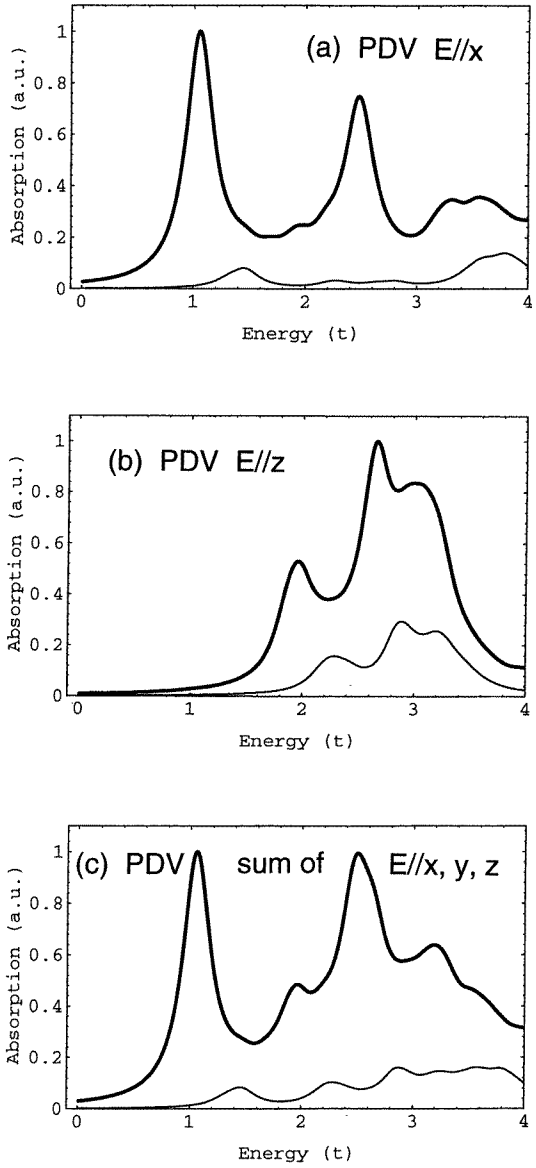

Figure 8. Optical absorption spectra of the PDV. The polymer is in the x–z plane, and its axis is parallel to the x-axis. The electric field of the light is parallel to the chain and in the direction of the x-axis in (a), and it is perpendicular to that axis and along the z-axis in (b). The orientationally averaged spectra are shown in (c). The number of PDV units is $N_{\rm m} = 9$. The bold line is for the total absorption. The thin line indicates the absorption of the long-range component. The Lorentzian broadening $\gamma = 0.15t$ is used.

is seen is smaller than that for PPV, due to the larger dimension of the monomer unit. The long-range component for the perpendicular-field case is larger than that for the parallel-field case. The long-range component for the orientationally averaged case saturates at $N_{\rm m} \sim 10$ with a value of approximately 11%. This polymer will be more photoconductive than PPV.

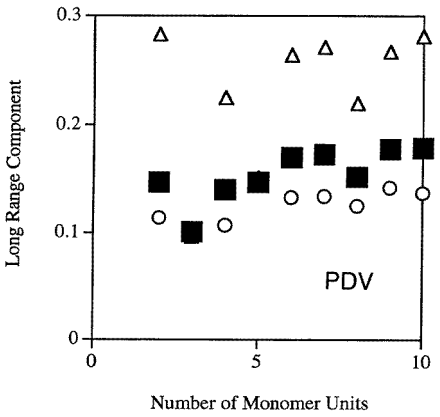

Figure 9. The long-range components of the optical absorption spectra as functions of the PDV unit number N_m. The squares are for the total absorption. The circles and triangles indicate the data for the cases with the electric field parallel and perpendicular to the polymer axis, respectively.

Table 1. The components of the long-range excitons in the four kinds of polymer for which we made calculations.

Polymer	Long-range component
PPP	7%
PPV	8%
PPD	11%
PDV	17%

3.3. PDV

In previous subsections, we have considered the series PPP, PPV, PPD, where the number of vinylene bonds increases in each monomer unit. There is another series—PPP, PPV, PDV (shown in figure 1(d))—where the number of phenyl rings increases in the monomer units. We consider the optical properties of PDV in this subsection.

Figure 8(a) shows the optical absorption spectra of the parallel-electric-field case. There are two main features: the lowest exciton peak at around $1.0t$, and the almost localized exciton feature at around $2.5t$. They are commonly seen in the polymers considered in this paper. The broad structure from $\sim 3t$ to $\sim 4t$ is due to the mixing of high-energy transitions among molecular orbitals with large energies in the presence of more phenyl rings. Figure 8(b) shows the spectra where the electric field is perpendicular to the polymer. In contrast to the parallel-field case, the spectral shape is rather similar to that for the other polymers. The long-range exciton contributions are remarkable in this case. Figure 8(c) shows the averaged spectra. The overall shape is like that of PPV shown in figure 4(c). There is a distinct lowest feature at around $1.0t$, and three small peaks are present at higher energies. However, the long-range component is larger than that of PPV. This polymer will show the strongest photoconductive properties among the polymers considered in this paper.

Finally, figure 9 shows the long-range components as functions of the number of monomer units. The long-range component of the perpendicular-field case is larger than

that of the parallel-field case, as is clearly seen in figure 8(b). The saturated value of the orientationally averaged spectra is approximately 17%. This is due to the complex molecular orbital structures of PDV. Table 1 summarizes the long-range components of the four polymers.

4. Summary

We have considered optical excited states of the electroluminescent polymers which are related to the best-known polymer, PPV. We have taken the long-range components of the optical excitations into consideration using the intermediate-exciton theory. The following are the main conclusions of this paper.

(1) As we go from PPP to PPV to PPD, the oscillator strengths of the long-range excitons become larger. Such a relative variation is explained by the difference between the numbers of vinylene bonds in each of the monomer units.

(2) The oscillator strengths of long-range excitons in PDV are much larger than those for the above three polymers, due to the increase in the number of phenyl rings.

(3) The energy positions of the almost localized excitons are nearly the same ($\sim 2.5t$) in the four polymers considered in this paper. The excitation energy of the almost localized exciton is just $2.0t$ in a free-electron model [9] for all the polymers. The enhancement of about $0.5t$ originates from the Coulomb interaction part of our model.

Acknowledgments

Useful discussions with Y Shimoi, S Abe, S Kobayashi, K Murata, and S Kuroda are acknowledged. Helpful communications with S Mazumdar, M Chandross, W Barford, D D C Bradley, R H Friend, E M Conwell, and Z V Vardeny are gratefully acknowledged. Numerical calculations were performed on the DEC AlphaServer of the Research Information Processing System Centre (RIPS), Agency of Industrial Science and Technology (AIST), Japan.

References

[1] Burroughes J H, Bradley D D C, Brown A R, Marks R N, Mackay K, Friend R H, Burn P L and Holmes A B 1990 *Nature* **347** 539
[2] Tessler N, Denton G J and Friend R H 1996 *Nature* **382** 695
[3] Hide F, Schwarz B J, Diaz-Garcia M A and Heeger A J 1996 *Chem. Phys. Lett.* **256** 424
[4] Pichler K, Halliday D A, Bradley D D C, Burn P L, Friend R H and Holmes A B 1993 *J. Phys.: Condens. Matter* **5** 7155
[5] Halliday D A, Burn P L, Friend R H, Bradley D D C, Holmes A B and Kraft A 1993 *Synth. Met.* **55–57** 954
[6] Murata K, Kuroda S, Shimoi Y, Abe S, Noguchi T and Ohnishi T 1996 *J. Phys. Soc. Japan* **65** 3743
[7] Harigaya K, Shimoi Y and Abe S 1996 *Proc. 2nd Asia Symp. on Condensed Matter Photophysics (Kobe, 1996)* p 25
[8] Harigaya K 1997 *J. Phys. Soc. Japan* **66** 1272
[9] Soos Z G, Etemad S, Galvão D S and Ramasesha S 1992 *Chem. Phys. Lett.* **194** 341
[10] Su W P, Schrieffer J R and Heeger A J 1980 *Phys. Rev.* B **22** 2099